Available online at www.sciencedirect.com
SCIENCE DIRECT®
Journal of Solid State Chemistry 177 (2004) 55–60
JOURNAL OF SOLID STATE CHEMISTRY
http://elsevier.com/locate/jssc

Characterization by X-ray diffraction, magnetic susceptibility and Mössbauer spectroscopy of a new alluaudite-like phosphate: $Na_4CaFe_4(PO_4)_6$

Mourad Hidouri,[a] Besma Lajmi,[a] Alain Wattiaux,[b] Léopold Fournés,[b] Jacques Darriet,[b] and Mongi B. Amara[a,*]

[a] *Laboratoire de Chimie Structurale des Matériaux, Département de Chimie, Faculté des Sciences, 5019 Monastir, Tunisia*
[b] *Institut de Chimie de la Matière Condensée de Bordeaux, CNRS 87, Avenue du Dr. A. Schweitzer, 33608 Pessac-Cedex, France*

Received 4 March 2003; received in revised form 6 May 2003; accepted 20 May 2003

Abstract

A single crystal of a new sodium calcium iron (III) phosphate, $Na_4CaFe_4(PO_4)_6$, has been synthesized by a flux method and characterized by X-ray diffraction, Mössbauer spectroscopy and magnetic susceptibility measurements. The compound crystallizes in the monoclinic space group $C2/c$($a = 12.099(5)$ Å, $b = 12.480(5)$ Å, $c = 6.404(2)$ Å, $\beta = 113.77(3)°$, $Z = 2$, $R_1 = 0.022$, $R_{w2} = 0.066$). The crystal structure belongs to the alluaudite type, characterized by the $X(2)X(1)M(1)M(2)_2(PO_4)_3$ general formula. The open framework results from Fe_2O_{10} units of edge-sharing FeO_6 octahedra, which alternate with $M(1)O_6$ octahedra ($M(1) = \frac{1}{2}Na + \frac{1}{2}Ca$) that form infinite chains. These chains are linked together through the common corners of PO_4 tetrahedra yielding two distinct tunnels of sodium cation occupation. This compound is antiferromagnetic with a Néel temperature of 35 K. Mössbauer parameters are consistent with the structural results.

Keywords: Phosphate; Alluaudite; X-ray diffraction; Magnetic susceptibility; Mössbauer spectroscopy

1. Introduction

Among the variety of $A_3M_2(XO_4)_3$ compounds, a large number exhibit $M_2(XO_4)_3$ three-dimensional frameworks built up by corner-sharing MO_6 octahedra and XO_4 tetrahedra, in which each tetrahedron is connected to four octahedra and each octahedron to six tetrahedra, the A cations occupying large sites in the interstitial space [1]. Suitable cationic replacements within such compounds may induce a transformation into several structural types and such evolutions can be correlated to the sizes of the substituting cations and the available sites of the involved structures. This phenomenon has already been observed in the case of the garnet-like arsenate $Na_3Fe_2(AsO_4)_3$ [2] in which the replacement of Na^+ by Ca^{2+} transforms its structure into the well-known alluaudite structure type [3,4].

The present work reports the synthesis and chara cterization by X-ray diffraction, Mössbauer spectroscopy and magnetic susceptibility measurements of $Na_4CaFe_4(PO_4)_6$. The alluaudite type structure of this compound shows that replacement of Na^+ by Ca^{2+} in the NASICON type iron phosphate $Na_3Fe_2(PO_4)_3$ [5] can also induce a transformation to the alluaudite type.

2. Experimental section

2.1. Synthesis

Crystals of $Na_4CaFe_4(PO_4)_6$ were grown in a flux of sodium molybdate. A mixture of 3.67 g of $Fe(NO_3)_3 \cdot 9H_2O$, 0.15 g of $CaCO_3$, 1.43 g of Na_2HPO_4 and 2.89 g of MoO_3 was introduced in a platinum crucible and subjected to the following thermal treatment: the mixture was heated at 400°C for 12 h to evolve the volatile decomposition products (NH_3, CO_2, H_2O) and then melted at 900°C for 1 h. The melted product was

*Corresponding author. Fax: +216-73-500-278.
E-mail address: mongi.benamara@fsm.rnu.tn (M.B. Amara).

0022-4596/03/$ - see front matter © 2003 Elsevier Inc. All rights reserved.
doi:10.1016/S0022-4596(03)00308-6

Table 1
Crystallographic data and structure refinement parameters for $Na_4CaFe_4(PO_4)_6$

Crystal data	
Formula unit	$Na_4CaFe_4(PO_4)_6$
SCD number	412964
Crystal system	Monoclinic
Space group	$C2/c$
a/Å	12.099(5)
b/Å	12.480(5)
c/Å	6.404(2)
β/deg	113.77(3)
V/Å^3	884.9(6)
Z	2
D_{cal}, D_{mes}/g cm^{-3}	3.47; 3.45(5)
Intensity measurements	
Crystal dimensions/mm	$0.20 \times 0.16 \times 0.12$
Apparatus	CAD_4 (Enraf–Nonius)
Wavelength	$\lambda(MoK\alpha) = 0.7107$ Å
Monochromator	Graphite
μ/mm^{-1}	4.28
Scan mode	$\omega/2\theta$
Scan speed	Variable
$2\theta_{max}$/deg	60
Background measuring time	$t_{max}/2$
Unique reflections, R_{int}	1277, 0.036
Retained reflections $[F_o > 4\sigma(F_o)]$	1268
Indices	$-16 \leqslant h \leqslant 15$, $-17 \leqslant k \leqslant 0$, $0 \leqslant l \leqslant 9$
$F(000)$	900
Structure solution and refinement	
Intensities correction	Lorentz-polarization effect
Resolution method	Direct method
Transmission factors	0.527–0.653
Agreement factors	$R_1 = 0.022$, $R_{w2} = 0.066$, $S = 1.281$ $[F_o^2 > 4\sigma(F_o^2)]$
Number of parameters	95
Extinction parameter	0.0054(4)
$(\Delta\rho)_{max}$, min/e Å^{-3}	1.068,−0.397
Weighting scheme	$W = 1/[\sigma^2(F_o^2) + (0.021P)^2 + 5.97P]$ where $P = [\max(F_o^2, 0) + 2F_c^2]/3$

cooled down to 500°C with a 10°C/h rate and then to room temperature with a 50°C/h rate. The crystals, obtained after washing with hot water to remove the flux, were brown with elongated forms. Qualitative elemental analysis on crystal samples using electron microprobe analysis indicated the presence of Na, Ca, Fe and P with no significant impurities.

2.2. Structure determination

A crystal of dimensions $(0.20 \times 0.16 \times 0.12)$ mm was selected for X-ray diffraction analysis. Data collection was performed with an Enraf–Nonius CAD4 X-ray diffractometer, equipped with graphite monochromated Mo$K\alpha$ radiation ($\lambda = 0.7107$ Å). A total of 3108 reflections were collected ($2\theta_{max} = 60°$) using the $\omega/2\theta$ scan mode. Of these 1277 are unique and 1268 were considered observed $[F_o^2 > 4\sigma(F_o^2)]$. The intensity data were corrected for Lorentz and polarization effects. An analytical absorption correction was applied after indexing the crystal faces ($T_{min} = 0.527$, $T_{max} = 0.653$). On the basis of lattice parameters, systematic absences and statistics of intensity distribution, the space group was determined to be the non-standard $I2/a$, the structure was however solved in corresponding standard space group $C2/c$. The iron atom positions were located by direct methods, using SIR-92 program [6] and the remaining atoms were found from successive Fourier difference maps. Atomic positions were refined by full-matrix least-squares method using SHELXL-97 program [7]. A final cycle refinement including atomic coordinates and anisotropic thermal parameters converged at $R_1 = 0.022$ and $R_{w2} = 0.066$ for the observed reflections. Crystal data, experimental conditions for intensity measurement, and refinement parameters are given in Table 1. Final atomic coordinates and equivalent isotropic temperature factors are reported in Table 2.

Table 2
Atomic coordinates and equivalent isotropic temperature factors in Å^2 (ESDs in parentheses)

Atom	Occupation	x/a	y/b	z/c	U_{eq}[a]
Fe	1	0.2240(1)	0.1559(1)	0.1400(1)	0.007(1)
$Na_{1/2}Ca_{1/2}$	1/2,1/2	0	0.2650(1)	1/4	0.015(1)
Na (1)	1	1/2	0	0	0.010(1)
Na(2)	1/2	0	0.0070(4)	3/4	0.035(1)
P(1)	1	0	0.2752(1)	3/4	0.005(1)
P(2)	1	0.2456(1)	−0.1034(1)	0.1335(1)	0.006(1)
O(11)	1	0.0525(2)	0.2038(2)	0.9632(3)	0.009(1)
O(12)	1	0.0962(2)	0.3498(2)	0.7284(3)	0.010(1)
O(21)	1	0.3767(2)	−0.0869(2)	0.1825(3)	0.015(1)
O(22)	1	0.1812(2)	0.0043(2)	0.1209(3)	0.012(1)
O(23)	1	0.1788(2)	−0.1620(2)	−0.0953(3)	0.009(1)
O(24)	1	0.2340(2)	−0.1738(2)	0.3263(3)	0.008(1)

[a] U_{eq} is defined as one-third of the trace of the orthogonalized U_{ij} tensor.

2.3. Magnetic and Mössbauer measurements

Magnetic susceptibility measurements were obtained using a Quantum Design SQUID MPMS-5S magnetometer operating at a constant applied magnetic field of 0.5 T in the temperature range 2–380 K.

Mössbauer measurements were performed using a constant acceleration HALDER-type spectrometer with a room temperature ^{57}Co source [Rh matrix] in transmission geometry. The polycrystalline absorbers containing about 10 mg/cm^2 of iron were used to avoid the experimental widening of the peaks. The spectra at 4.2 and 293 K were recorded using a variable temperature cryostat. The velocity was calibrated using pure iron metal as the standard material. The refinement of the Mössbauer spectra showed an important and abnormal widening of the peaks, so that the spectra have been fitted assuming a distribution either of quadrupolar splittings ($T = 293$ K) or/and of hyperfine fields ($T = 4.2$ K).

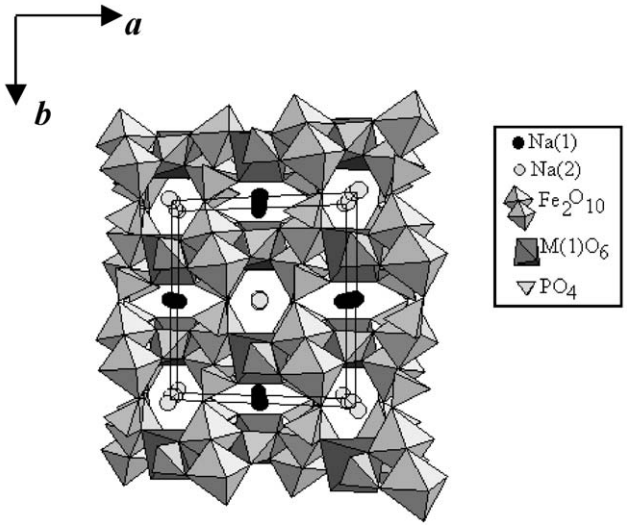

Fig. 1. A perspective view of the $Na_4CaFe_4(PO_4)_6$ structure along the [001] direction.

3. Results and discussion

3.1. Structural description

The $Na_4CaFe_4(PO_4)_6$ structure as viewed along the *c*-axis is shown in Fig. 1. This structure is built up from Fe_2O_{10} units of edge-sharing FeO_6 octahedra, which alternate with $M(1)O_6$ octahedra ($M(1) = \frac{1}{2}Na + \frac{1}{2}Ca$) that form infinite chains running along $[10\bar{1}]$ direction (Fig. 2b). Equivalent chains are linked together through the corners of PO_4 tetrahedra. The $P(1)O_4$ tetrahedron connects two chains by sharing each pair of its oxygen with one chain. The $P(2)O_4$ tetrahedron links three adjacent chains and thus two of its oxygen atoms belong to the same chain. In this way the three-dimensional framework leads to two types of tunnels at $x = \frac{1}{2}$, $y = 0$ and $x = 0$, $y = 0$ which are occupied by the sodium atoms Na(1) and Na(2), respectively.

Table 3 lists interatomic distances around various coordination environments in $Na_4CaFe_4(PO_4)_6$. The iron coordination environment has a very distorted octahedral geometry, as shown by the Fe–O bond distance values between 1.953(2) and 2.175(2) Å. The O–Fe–O bond angles vary between 79.71(7) and 105.70(8)° and between 161.97(8) and 176.71(7)° for the *cis* and the *trans* angles, respectively. This distortion is probably due to the rigidity of PO_4 units surrounding the Fe atom (Fig. 2a). The average Fe–O bond length of 2.031 Å is however in a good agreement with the predicted value of 2.03 Å for Fe^{3+} in an octahedral environment [8].

The two crystallographic distinct PO_4 tetrahedra contained in this structure have an identical P–O mean distance of 1.538 Å which is in a good agreement with those typically observed in phosphates without hydrogen bonding [9–14]. Atom P(1) sits on a 2-fold axis and thus it has a more symmetric environment than P(2) which sits in a general position.

The coordination number of each cationic site was determined assuming a cation-oxygen distances below 3.0 Å. The coordination polyhedron of the ($Na_{1/2}$,$Ca_{1/2}$) site is a distorted octahedron with three cation-oxygen bond lengths ranging from 2.303(2) to 2.363(2) Å. The

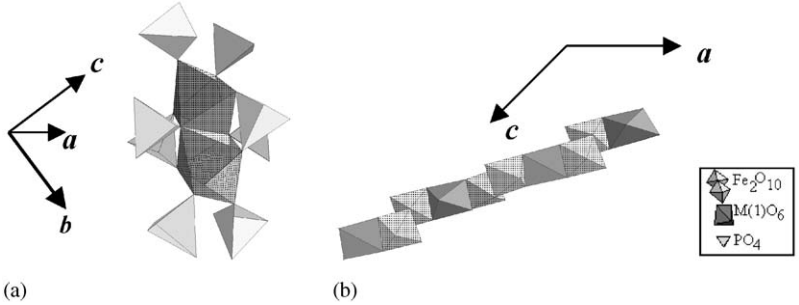

Fig. 2. (a) Polyhedral environment of Fe in $Na_4CaFe_4(PO_4)_6$. (b) View of the infinite chains of alterning Fe_2O_{10} units and $M(1)O_6$ octahedra.

Table 3
Selected interatomic distances (Å) in $Na_4CaFe_4(PO_4)_6$

Fe–O(22) 1.953(2)	P(1)–O(11)	1.537(2) × 2	P(2)–O(21)	1.502(2)
Fe–O(23) 1.981(2)	P(1)–O(12)	1.540(2) × 2	P(2)–O(22)	1.539(2)
Fe–O(12) 1.992(2)	<P(1)–O>	1.538	P(2)–O(23)	1.543(2)
Fe–O(11) 2.013(2)			P(2)–O(24)	1.567(2)
Fe–O(24) 2.073(2)			<P(2)–O>	1.538
Fe–O(24)′ 2.175(2)				
<Fe–O> 2.031				
(Na, Ca) site environments				
$(Na_{1/2}Ca_{1/2})$–O(11)	2.303(2) × 2	Na(1)–O(21)		2.256(3) × 2
$(Na_{1/2}Ca_{1/2})$–O(21)	2.304(2) × 2	Na(1)–O(12)		2.374(2) × 2
$(Na_{1/2}Ca_{1/2})$–O(23)	2.363(2) × 2	Na(1)–O(21)′		2.484(2) × 2
$<Na_{1/2}Ca_{1/2}>$–O>	2.323	<Na(1)–O>		2.371
Na(2)–O(22)	2.501(2) × 2			
Na(2)–O(22)′	2.640(2) × 2			
Na(2)–O(11)	2.757(4) × 2			
Na(2)–O(23)	2.895(4) × 2			
<Na(2)–O>	2.698			

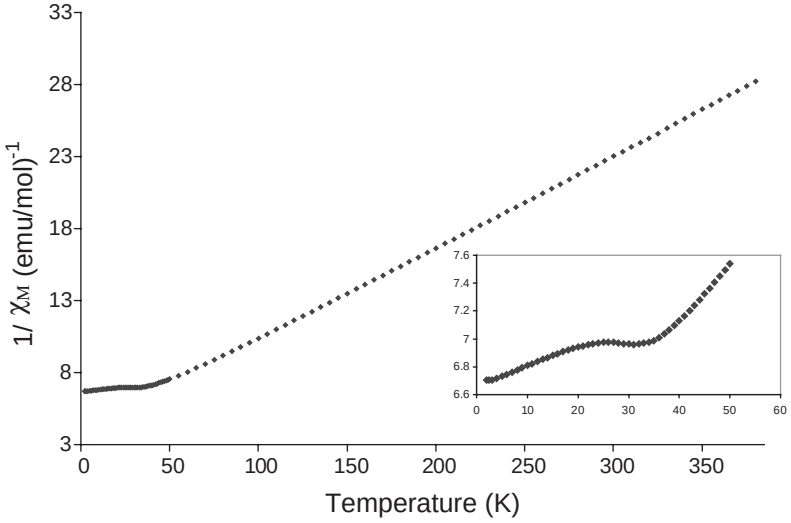

Fig. 3. Temperature dependence of the inverse molar magnetic susceptibility of $Na_4CaFe_4(PO_4)_6$.

Na(1) site environment is also a highly distorted octahedron, with three Na(1)–O bond distances scattering from 2.256(3) to 2.484(2)Å. Na(2) site environment is a distorted cube with Na(2)–O bond distances between 2.501(2) and 2.895(4)Å.

The crystal structure of $Na_4CaFe_4(PO_4)_6$ is closely related to the alluaudite type structure of the synthesized mixed valent iron phosphates: $NaFe_3(PO_4)_3$ [10], $Na_2Fe_3(PO_4)_3$ [11] and $NaFe_{3.67}(PO_4)_3$ [12] with one main difference being the presence of separated Fe_2O_{10} units of edge-sharing FeO_6 octahedra.

In terms of the $X(2)X(1)M(1)M(2)_2(PO_4)_3$ general formula of the alluaudite, the $M(1)$ and $M(2)$ environments have both an octahedral geometry. These octahedra share their edges with each other to form infinite chains running along the [10−1] direction. In the alluaudite iron phosphates, synthesized so far either $M(1)$ and $M(2)$ are occupied by iron atoms and thus the chains are formed by iron octahedra only [10–12]. In the title compound structure the $M(2)$ site is occupied by Fe while $M(1)$ contains a statistical distribution of Na and Ca. The chains characterizing the alluaudite structure are then built up from Fe_2O_{10} units alterning with $(Na_{1/2},Ca_{1/2})O_6$ octahedra.

3.2. Magnetic susceptibility

A plot of the inverse molar magnetic susceptibility $1/\chi_M$ of $Na_4CaFe_4(PO_4)_6$, for the temperature range (2–380 K) is shown in Fig. 3. This compound exhibits an antiferromagnetic behavior with a Néel temperature of 35 K and a Curie–Weiss parameter θ of −61.5 K. The

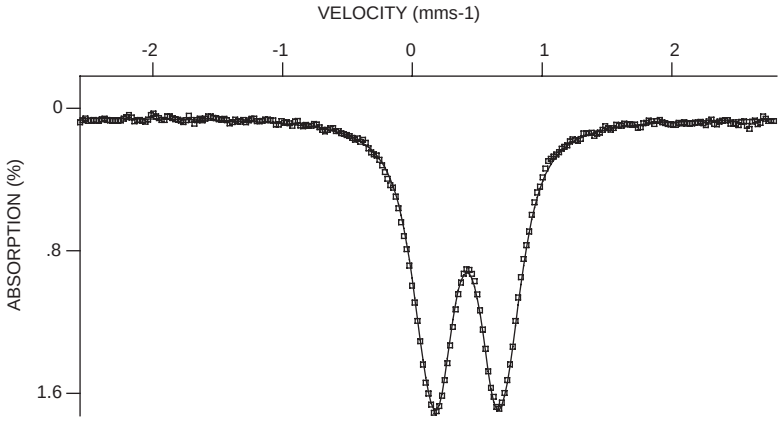

Fig. 4. Room temperature Mössbauer spectrum.

Curie constant C and the effective magnetic moment per Fe center ($3.93\,\mathrm{emu\,K^{-1}}$ and $5.61\mu_B$, respectively) are slightly low but consistent with the assignment of high-spin Fe^{3+} (d^5) in octahedral environment.

3.3. Mössbauer spectroscopy

3.3.1. Room temperature

A Mössbauer characterization was performed at room temperature for $Na_4CaFe_4(PO_4)_6$ phase (Fig. 4). The Mössbauer spectrum consists of a symmetric single quadrupole doublet which was fitted to two lorentzian profile lines by the least-squares method. This first mathematical treatment shows only Fe^{3+} ions in the high-spin state when octahedral environments are present. Nevertheless, the large value of the line width suggests the existence of a distribution of quadrupolar splittings and therefore of local iron environments. According to the structural study, $M(1)$ site is occupied by Na^+ or Ca^{2+} cations which induces the existence of two different iron neighborhoods. In those conditions, the Mössbauer spectra was fitted by considering two distributions of quadrupolar splittings with a constant value of the line width ($\Gamma = 0.28\,\mathrm{mm\,s^{-1}}$) for the ^{57}Fe isotope and the isomer shift fixed at the value preliminary determined in the first mathematical treatment. The hyperfine parameters for each distribution are listed in Table 4. This shows that the difference in surrounding due to the distribution of Na^+ and Ca^{2+} within $M(1)$ is detected by Mössbauer spectroscopy in agreement with the X-ray study. For the two distributions (DS(1) and DS(2)), these hyperfine parameters are typical of iron (III) in a distorted octahedral environment. Since average quadrupolar splitting Δ_1 is clearly smaller than Δ_2, we can deduce that the environment corresponding to DS(1) is more regular than that the environment relating to DS(2). Moreover their populations are nearly equal as predicted by X-ray diffraction study.

Table 4
Mössbauer parameters for $Na_4CaFe_4(PO_4)_6$ at 293 K

Distribution	δ (mm/s)	$<\Delta>$ (mm/s)	Γ (mm/s)	% population
DS(1)	0.432	0.436	0.280	49.6
DS(2)	0.430	0.611	0.280	50.4

Table 5
Mössbauer parameters for $Fe_2(SO_4)_3$, $Na_3Fe_2(PO_4)_3$, $Na_4CaFe_4(PO_4)_6$, $Fe_2(MoO_4)_3$ and $FeAsO_4$

Compound	δ (mm/s)	Δ (mm/s)	Γ(mm/s)	Ref.
$Fe_2(SO_4)_3$	0.49	0.32	0.43	[15]
$Na_3Fe_2(PO_4)_3$	0.45(1)	0.31(1)	0.28(1)	[16]
$Na_4CaFe_4(PO_4)_6$				
Distribution 1	0.432	0.436	0.28	This study
Distribution 2	0.430	0.611	0.28	
$Fe_2(MoO_4)_3$	0.41(1)	0.20(1)	0.28	[17]
$FeAsO_4$	0.30	0.54		[18]

The value of the paramagnetic isomer shift of $Na_4CaFe_4(PO_4)_6$ can be compared to that of related compounds $Fe_2(SO_4)_3$ [15], $Na_3Fe_2(PO_4)_3$ [16], $Fe_2(MoO_4)_3$ [17] and $FeAsO_4$ [18] (Table 5) whose structures are build up from corner-sharing FeO_6 octahedra and XO_4 tetrahedra (X = S, P, Mo, As). An increase is observed in the sense $\delta_{As} < \delta_{Mo} < \delta_P < \delta_S$. This trend likely corresponds to an increase of the ionic character of the Fe–O bond as a consequence of increasing covalence of the antagonistic bond X–O from arsenate to sulfate.

3.3.2. T=4.2 K

The Mössbauer spectrum at $T = 4.2$ K shows clearly a sextuplet characteristic of the magnetic ordered compound (Fig. 5) in agreement with the magnetic susceptibility results. Due to the line width broadening of the peaks the refinement was done using only one

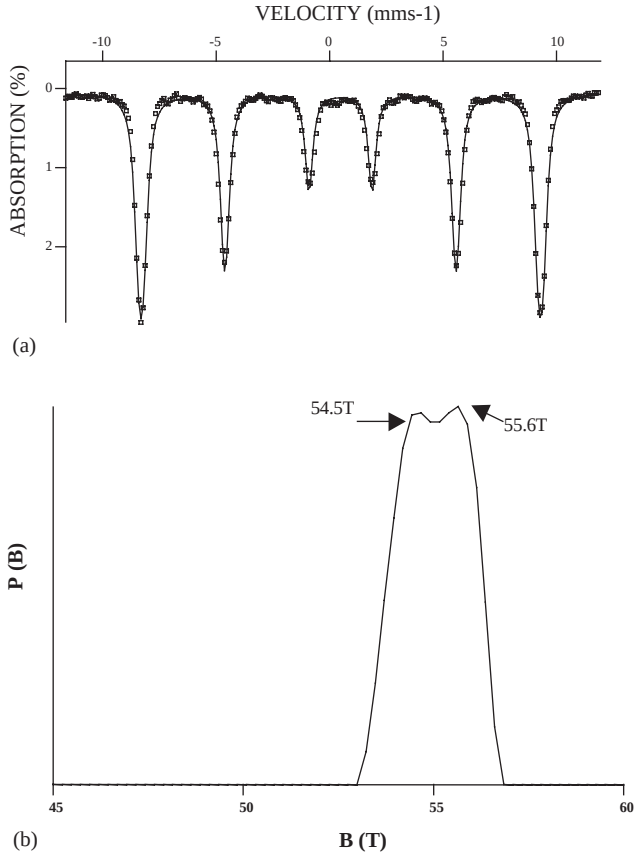

Fig. 5. Mössbauer spectrum (a) and corresponding hyperfine field distribution (b) for $Na_4CaFe_4(PO_4)_6$ at 4.2 K.

Table 6
Mössbauer parameters for $Na_4CaFe_4(PO_4)_6$ at 4.2 K

δ (mm/s)	Γ (mm/s)	ε (mm/s)	B (T)
0.539	0.40	+0.008	55.0

hyperfine field distribution. The results are given in Table 6.

The values of the average hyperfine field ($B = 55$ T) and the isomer shift [$\delta = 0.539\,\mathrm{mm\,s^{-1}}$) are in a good agreement with the values observed for α–$Li_3Fe_2(PO_4)_3$ ($B = 54.9$ T, $\delta = 0.546$ mm/s) [19]. However, this result seems to contradict the interpretation proposed for $T = 293$ K where two quadrupolar splitting distributions have been considered. Nevertheless, if one consider such distribution, the values of the two hyperfine fields $B1 = 54.5$ T and $B2 = 55.6$ T are close and of same intensity (Fig. 5b) which is in good agreement with the results at $T = 293$ K and confirms the existence of two very close iron environments.

The difference between the low temperature and the room temperature isomer shifts ($\Delta(\delta) \approx 0.12$ mm/s) is due in part to the second order Doppler effect.

4. Conclusions

$Na_4CaFe_4(PO_4)_6$ has been prepared and crystallizes with the alluaudite type structure. Its main feature, compared to other synthetic alluaudite-like phosphates is the existence of isolated Fe_2O_{10} units of edge-sharing FeO_6 octahedra alternating with $(Na_{1/2},Ca_{1/2})O_6$ octahedra to form infinite chains. Magnetic susceptibility measurements have shown that the studied compound is antiferromagnetic with a Néel temperature of 35 K. The Mössbauer spectroscopy confirms the trivalent state for Fe and the highly distortion in the FeO_6 octahedron, predicted by the X-ray study.

Acknowledgments

The authors thank Pr. M. Rzeigui of the Sciences University of Bizerte, Tunisia, for the single crystal XRD measurements.

References

[1] A. Jouanneaux, A. Verbaere, Y. Piffard, A.N. Fitch, M. Kinoshita, Eur. J. Solid State Inorg. Chem. 28 (1991) 683–699.
[2] S. Khorari, A. Rulmont, P. Tarte, J. Solid State Chem. 137 (1998) 112–118.
[3] P.B. Moore, Am. Mineral. 56 (1971) 1955–1975.
[4] D.J. Fisher, Am. Mineral. 40 (1955) 1100.
[5] M. Pintard-Scrépel, F. d'Yvoire, F. Rémy, C. R. Acad. Sc. Paris 286C (1978) 381–383.
[6] A. Altomare, G. Cascarano, C. Giacovazzo, A. Guagliardi, J. Appl. Crystallogr. 26 (1993) 343–350.
[7] G.M. Sheldrick, SHELXL97, A Program for the Solution of the Crystal Structures, University of Göttingen, 1997.
[8] R.D. Shannon, Acta Crystallogr. 32 (1976) 751–764.
[9] K.H. Lii, J. Ye, J. Solid State Chem. 131 (1997) 131–137.
[10] D.R. Corbin, J.F. Whitney, W.C. Fulz, G.D. Stucky, M.M. Eddy, A.K. Cheetham, Inorg. Chem. 25 (1986) 2279–2280.
[11] O.V. Yakubovich, M.A. Simonov, Y.K.E. Tismenko, N.V. Belov, Dokl. Acad. Nauk. SSSR 236 (1977) 1123–1126.
[12] M.B. Korzenski, G.L. Schimek, J.W. Kolis, G.J. Long, J. Solid State Chem. 139 (1998) 152–160.
[13] T.E. Warner, W. Milius, J. Maier, J. Solid State Chem. 106 (1993) 301–309.
[14] P. Feng, X. Bu, G.D. Stucky, J. Solid State Chem. 129 (1997) 328–333.
[15] G.J. Long, G. Longworth, P. Battle, A.K. Cheetham, R.V. Thundathil, D. Beveridge, Inorg. Chem. 18 (1979) 624–632.
[16] D. Beltran-Porter, R. Olazcuaga, L. Fournes, F. Menil, G. Le Flem, Rev. Phys. Appl. 15 (1980) 1155–1160.
[17] Z. Jirack, R. Salmon, L. Fournes, F. Menil, P. Hagenmuller, Inorg. Chem. 21 (1982) 4218–4223.
[18] W.M. Reiff, M.J. Kwiecien, R.J.B. Jakeman, A.K. Cheetham, C.C. Torardi, J. Solid State Chem. 107 (1993) 401–412.
[19] A. Goni, L. Lezama, N.O. Horero, L. Fournes, R. Olazcuaga, G.E. Barberis, T. Rojo, Chem. Mater. 12 (2000) 62–66.